New Craniodental Materials of *Litolophus gobiensis* (Perissodactyla, "Eomoropidae") from Inner Mongolia, China, and Phylogenetic Analyses of Eocene Chalicotheres

BIN BAI,[1,2] YUANQING WANG,[1] AND JIN MENG[3]

ABSTRACT

We describe new craniodental specimens of *Litolophus gobiensis* recently unearthed from the type locality of the genus, and conduct phylogenetic analyses of Eocene chalicotheres based on a data matrix containing 21 taxa and 58 craniodental characters. Although the phylogenetic relationships of the Eocene chalicotheres are not well resolved in the strict component consensus tree, the 50% majority rule consensus shows that two post–earliest Eocene chalicothere lineages are present. The first lineage represents the main line of chalicothere evolution, including "*Grangeria*" *anarsius*, *Eomoropus*, and post-Eocene chalicotheres. The second lineage, consisting of *Litolophus gobiensis* and *Grangeria canina*, is the sister group and stem member to the main lineage. The derivative strict reduced consensus tree, with three unstable taxa pruned, supports some tree topologies of the 50% majority consensus. The taxonomy of some chalicothere taxa is revised based on the phylogenetic analyses, such as "*Grangeria*" *anarsius* being probably better referred to the genus *Eomoropus* as originally identified, *E. ulterior* being the sister taxon to *E. amarorum*, and *Lophiodon* being excluded from the Ancylopoda but allied with the Ceratomorpha.

INTRODUCTION

Chalicotheres, at least some advanced forms, are commonly regarded as a unique perisso- dactyl group characterized by bearing clawed ungual phalanges instead of hooves. Chali- cotherioidea is traditionally divided into two families: Eomoropidae and Chalicotheriidae,

[1] Key Laboratory of Evolutionary Systematics of Vertebrates, Institute of Vertebrate Paleontology and Paleoanthropology, Chinese Academy of Sciences, P.O. Box 643, Beijing 100044, P.R. China (baibin@ivpp.ac.cn and wangyuanqing@ivpp.ac.cn).
[2] Graduate School of the Chinese Academy of Sciences, Beijing 100039.
[3] Division of Paleontology, American Museum of Natural History, New York (jmeng@amnh.org).

although the former is probably a paraphyletic group (Coombs, 1989, 1998). Colbert (1934) described the Eocene chalicothere species "*Grangeria*" *gobiensis* based on several skulls, mandibles, fore- and hind feet, and some caudal vertebrae from the locality near Camp Margetts, 25 miles southwest of Iren Dabasu, Inner Mongolia, China. The horizon bearing "*G.*" *gobiensis* was considered the "Irdin Manha Formation" at the time. Radinsky (1964a) proposed a new genus *Litolophus* for "*G.*" *gobiensis*, and specified the holotype locality as 6 miles west of Camp Margetts, about 27 miles southwest of Iren Dabasu. He, however, questioned the correlation and age determination of the "Irdin Manha Formation" at the locality (Radinsky, 1964b).

Recently, new materials of this species were unearthed from Nuhetingboerhe, Erlian Basin, Inner Mongolia, China. The field investigation clarified some uncertainties about the stratigraphy of the region as raised by Radinsky (1964b) and demonstrated that Nuhetingboerhe is the same area where the holotype of *Litolophus gobiensis* was found. The recent study also shows that the strata containing the *Litolophus* specimens are the basal Arshanto Formation rather than the Irdin Manha Formation and are of Early Eocene in age (Meng et al., 2007b; Sun et al., 2009). All materials were collected from the "chalicothere pit" quarry during several field seasons in the last few years. The quarry produced several skulls, more than 20 mandibles, and a large number of skeletal specimens of *Litolophus gobiensis*. Although these materials are distorted to different degrees, they show important features that are previously unknown or unclear for the species. From the same site, numerous specimens of other mammals have been collected. Among them the lagomorph *Dawsonolagus antiquus*, the rodent *Archetypomys erlianensis* and *Erlianomys combinatus*, and the dinoceratan *Gobiatherium mirificum* have been described (Bai, 2006; Li et al., 2007; Li and Meng, 2010; Meng et al., 2007a). Several new rodents, insectivores, and the primitive rhinocerotoid *Hyrachyus* will be reported in future studies. Here we describe the new craniodental material of *L.*

gobiensis and, based on the new specimens and published ones, conduct phylogenetic analyses for Eocene chalicotheres. The postcranial specimens will be described in a separate study.

MATERIALS AND METHODS

For convenience, Eomoropidae is still adopted in this study although the taxon is probably paraphyletic. In addition, there is currently no working phylogeny for taxa included in Eomoropidae and their relationships with Chalicotheriidae. The dental terminology used here (fig. 1) is modified from Coombs (1978a), Hooker (1994), and Qiu and Wang (2007). The terminology for upper cheek teeth is basically consistent in perissodactyls, but that for lower cheek teeth was often used inconsistently by different authors (Qiu and Wang, 2007). In this paper, two primarily transverse lophids in the lower molars are called metalophid and hypolophid as originally used by Osborn (1907). The crest connecting the protoconid and metaconid is the metalophid, and the one connecting the hypoconid and entoconid is the hypolophid. Because the trigonid on unworn teeth of *Litolophus* is nearly U-shaped, the lophid extending from the protoconid anterolingually is called the protolophid, and the lophid extending from the paraconid buccally is called the paralophid, as proposed by Qiu and Wang (2007). For the talonid, the lophid extending from the hypoconid anterolingually is called the cristid obliqua (Zhou et al., 1975). The terminology for upper cheek teeth follows Coombs (1978a), except using paraconule instead of protoconule. Log-ratio diagrams were plotted for comparisons of tooth dimensions using the method described in Simpson (1941).

INSTITUTIONAL ABBREVIATIONS: AMNH, American Museum of Natural History, New York; IVPP: Institute of Vertebrate Paleontology and Paleoanthropology, Beijing; SDM: Shandong Provincial Museum, Jinan, Shandong Province, China; USNM: United States National Museum of Natural History, Smithsonian Institution, Washington, D.C.; VM: Geological Museum of China, Beijing.
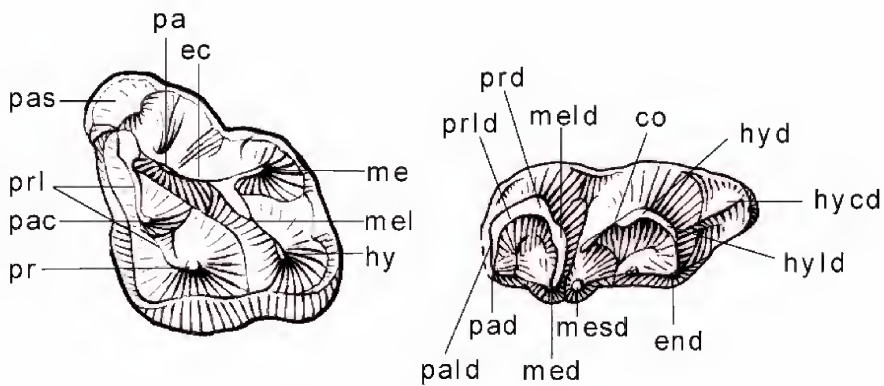
Fig. 1. Diagrammatic M3 and m3 of *Litolophus gobiensis*, showing dental structures mentioned in the text. Abbreviations: **co**, cristid obliqua; **ec**, ectoloph; **end**, entoconid; **hy**, hypocone; **hycd**, hypoconulid; **hyd**, hypoconid; **hyld**, hypolophid; **me**, metacone; **med**, metaconid; **mel**, metaloph; **meld**, metalophid; **mesd**, "metastylid"; **pa**, paracone; **pac**, paraconule; **pad**, paraconid; **pald**, paralophid; **pas**, parastyle; **pr**, protocone; **prd**, protoconid; **prl**, protoloph; **prld**, protolophid.

SYSTEMATIC PALEONTOLOGY

Order PERISSODACTYLA Owen, 1848

Superfamily CHALICOTHERIOIDEA Gill, 1872

Family EOMOROPIDAE Gill, 1872

Genus *LITOLOPHUS* Radinsky, 1964

LITOLOPHUS GOBIENSIS (Colbert), 1934

HOLOTYPE: AMNH 26645. A crushed skull and a mandible, probably belonging to the same individual (Colbert, 1934).

PARATYPES: AMNH 26644, 26646–26649, 26653–26659. Skulls, mandibles, forefeet and hind feet found in a small quarry, 6 miles west of Camp Margetts, Inner Mongolia.

REFERRED SPECIMENS: IVPP V16139, a relatively well-preserved skull with right P2–M3 and left C–M3; V16140-1, a greater part of right side of a skull with P1–4 and M3; V16141-1, a posterior portion of a skull with right P2–M1, M3 and left P2–4, M2–3; V16141-2, a right side of the anterior portion of a skull; V16142, a dorsoventrally compressed subadult skull with P2–M3; V16143, a fragmentary premaxilla with I3; V16144.1, a right I2; V16144.2, a left I2; V16144.3, a left I2; V16144.4, a right I3; V16147, a subadult mandible with right p3–m3 and left i1, p2–m3;

V16148, a partial subadult left lower mandible with p3–m3 and two i1s; V16149, a nearly complete mandible with c–m3; V16150, a nearly complete mandible with p2–m3; V16167.1, a right i2; V16167.2, a right i2; V16167.3, a right i2; V16167.4, a left i3; V16167.5, a left i3.

EMENDED DIAGNOSIS: Medium-sized chalicotheres with low-crowned teeth; dental formula 3·1·4·3/3·1·3·3; a short diastema present between P1 and P2; P3–4 metalophs joining the ectolophs in a low position, and paraconules usually well developed; upper molars with prominent parastyles and paraconules, but lacking mesostyles; paracones and metacones on upper molars nearly vertically implanted, protocones posteriorly extended, and metalophs oblique and relatively short; M3 metaloph and metacone posterobuccally rotated; lower molar cristid obliqua anterolingually directed to the buccal sides of the "metastylids," and the hypolophids oblique; posterior cingulids on m1–2 raised upward but lacking the cuspate hypoconulids; m3 with a well-developed hypoconulid lobe; parietal crests gently contracted behind postorbital processes; supraorbital foramen absent; paroccipital process slender and completely separated from the relatively broader and larger posttympanic process; posterior border of the palate nearly U-shaped at the level of posterior edge of M3; ventral surface of the

promontorium smooth; deep fossa for the stapedius muscle present; mandible long and slender, with long shallow symphysis and high ascending ramus; angular process of the mandible with a nearly semicircular border.

LOCALITY AND HORIZON: Nuhetingboerhe, Erlian Basin, Inner Mongolia, China. Lower part of the Arshanto Formation; early Arshantan (Early Eocene).

DESCRIPTION

SKULL: The anterior part of the premaxilla is stout and curves ventroanteriorly. Three appressed alveoli for incisors are present on each side of the premaxillae, and I3 is separated from the canine by a considerable diastema. A ridge extends anteroposteriorly on the ventral surface of the anterior part of the premaxilla and almost fades out near the lingual side of I2 (fig. 2A). The premaxilla contacts the nasal for a long distance (ca. 45 mm on V16141-2), so that the nasal notch is not retracted, and the posterior border of the nasal notch is probably above the canine. The maxilla is broad (fig. 2B). The small infraorbital foramen opens above P3. The nasals are long and flat, and the posterior portions expand laterally (fig. 2C).

The frontal is flat, with a stout postorbital process of the frontal where the supraorbital foramen is absent. The dorsal orbit has a rough boundary, while the postorbital process of the jugal is more posteriorly placed than that of the frontal, and the ventral boundary of the orbit is smooth. The relatively small orbit lies above M3 and is open behind. The end of the jugal bone of V16141-1 forms a dorsoventrally compressed plate just in front of the glenoid fossa.

The parietal crests do not contract abruptly behind the postorbital processes of the frontals, and they converge into a sagittal crest at the level of the postglenoid process. The long and sharp sagittal crests of V16139 and V16140-1 elevate posteriorly to some extent, while that of V16141-1 extends horizontally posteriorly (fig. 3). The difference probably implies sexual dimorphism, but the distortion of V16139 and V16140-1 may also account for the elevated sagittal crest. On the medioinferior portion of the parietals of V16141-1 are a number of nutrient foramina.

V16141-1 preserves several small foramina on the dorsal surface of the lateral portion of the zygomatic process of the squamosal. The lower border of the zygomatic arch is almost straight. The dorsal boundary of the zygomatic arch behind the orbit rises posteriorly rapidly, and meets the sharp occipital crest through the short temporal crest. The glenoid fossa is flat and roughly trapezoidal in outline. The postglenoid process of V16141-1 is massive and transversely extended (fig. 3), nearly perpendicular to the long axis of the skull. In contrast, although the postglenoid process of V16139 is broken, it seems much slenderer (fig. 2B).

The foramen ovale is medial to the glenoid fossa and opens anteroventrally, separate from the medial lacerate foramen (fig. 2A). The large posterior opening of the alisphenoid canal is anteromedial to the foramen ovale and opens lateroventrally. The long axes of these openings are nearly perpendicular to each other.

The outline of the occipital side is triangular (fig. 4). The occipital crest is sharp, extending broadly ventrally to join the temporal crest. The nuchal ligament depression appears narrow and deep. The foramen magnum is rhombic with rounded corners, and its width is greater than the height. The occipital condyles have slightly convex outer surfaces. The paroccipital process is slender and short, and is completely separated from the relatively broader and larger posttympanic process (this condition is better preserved on V16141-1). The paroccipital process has a flat anterior surface, whereas its posterior surface is concave longitudinally and convex latitudinally. The posterior region of the basioccipital bone is composed of slightly convex medial and semicircular lateral facets.

The suture between the basisphenoid and presphenoid bones is obliterated. The posterior border of the palate is nearly U-shaped and located at the posterior edge of M3.

The right petrosal of V16139 is well preserved (fig. 5). The surface of the promontorium is smooth and flat, on which the fenestra ovalis and fenestra rotunda are located posterolaterally. The fenestra ovalis opens ventrally, and is separated from the promontorium by a weak ridge. A very small
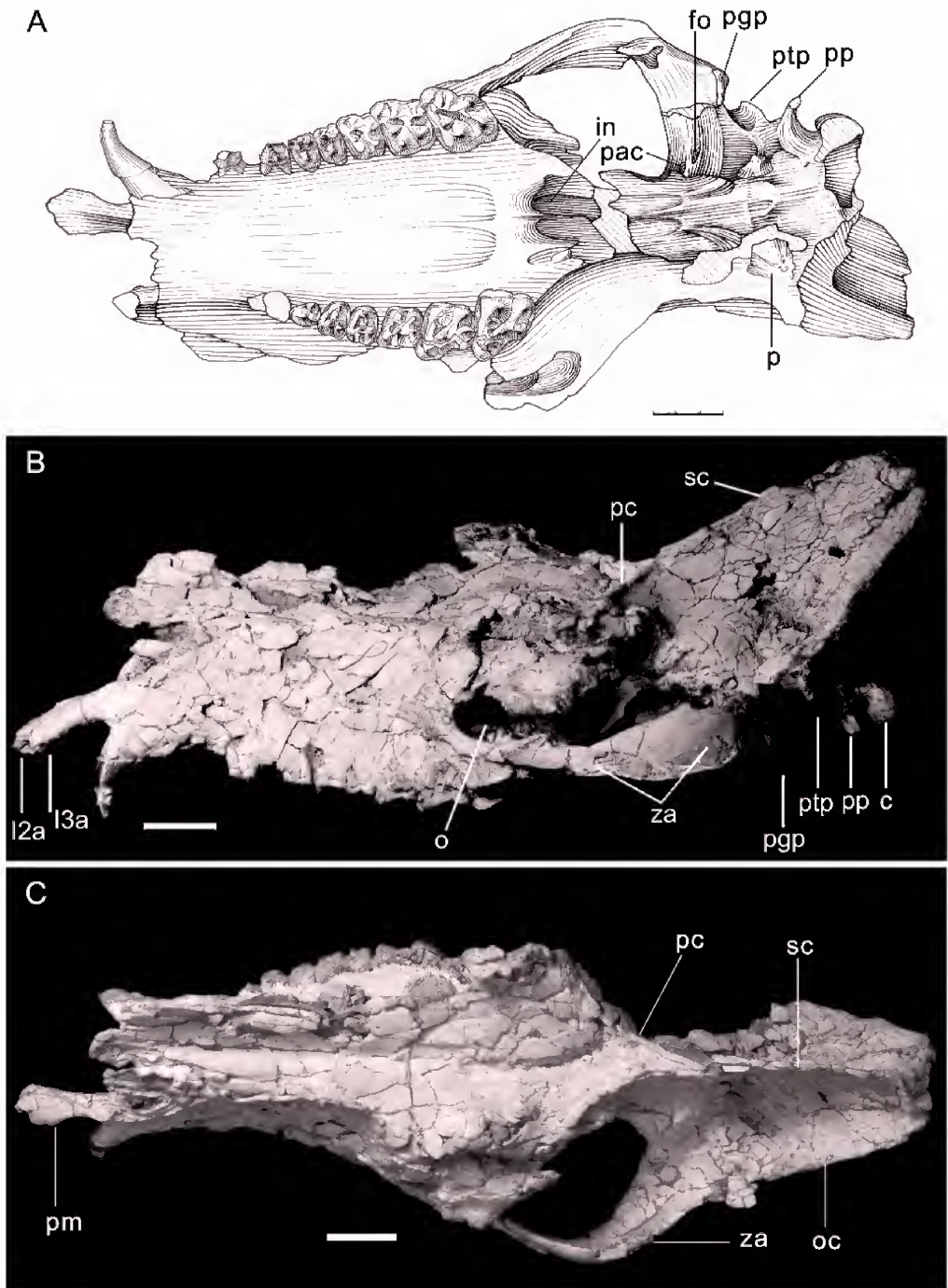
Fig. 2.   Skull of *Litolophus gobiensis* (IVPP V16139). (A) Ventral view, (B) left lateral view, and (C) dorsal view. Abbreviations: **c,** occipital condyle; **fo,** forman ovale; **in,** internal naris; **o,** orbit; **oc,** occipital crest; **p,** petrosal; **pac,** posterior opening of the alisphenoid canal; **pc,** parietal crest; **pgp,** postglenoid process; **pm,** premaxilla; **pp,** paroccipital process; **ptp,** posttympanic process; **sc,** sagittal crest; **za,** zygomatic arch; **I2a**: I2 alveolus; **I3a**: I3 alveolus. Scale = 3 cm.
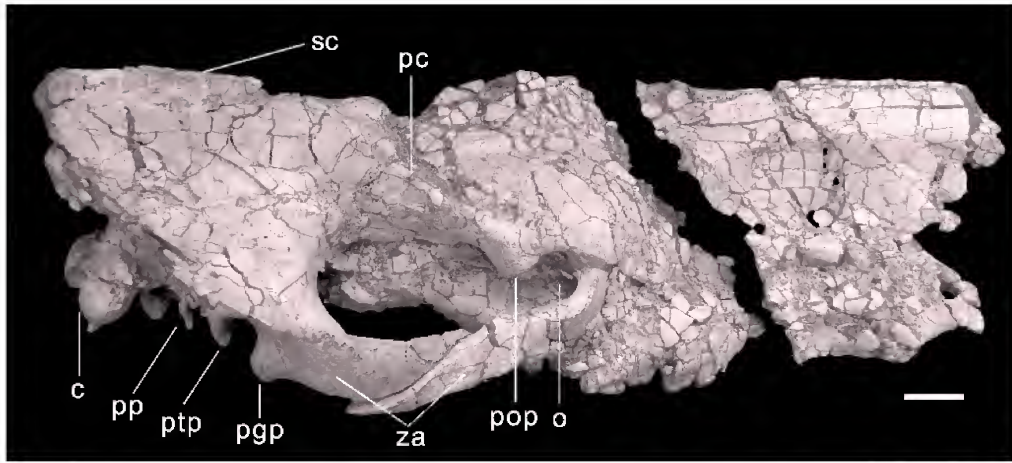
Fig. 3.   Right lateral view of the skull of *Litolophus gobiensis* (IVPP V16141-1, V16141-2). Abbreviation: **pop**: postorbital process; see legend for figure 2 for other abbreviations. Scale = 3 cm.

foramen, possibly a nutrient foramen as in *Heptodon posticus* (Radinsky, 1965), is present lateral to the fenestra ovalis. Anterior to the fenestra ovalis, a relatively long groove is present along the lateral border of the petrosal. This groove is probably the tympanic aperture of the facial canal. The posteriorly opening fenestra rotunda is located postero-medial to the fenestra ovalis and is larger than the latter. A deep fossa located posterolateral

to the fenestra ovalis is for the stapedius muscle. The tympanic bone is probably present, as deduced from lamellar bones present lateral to the left petrosal of V16139 and the right petrosal of V16141-1. The posttympanic process does not fuse with the postglenoid process at its extremity, so it does
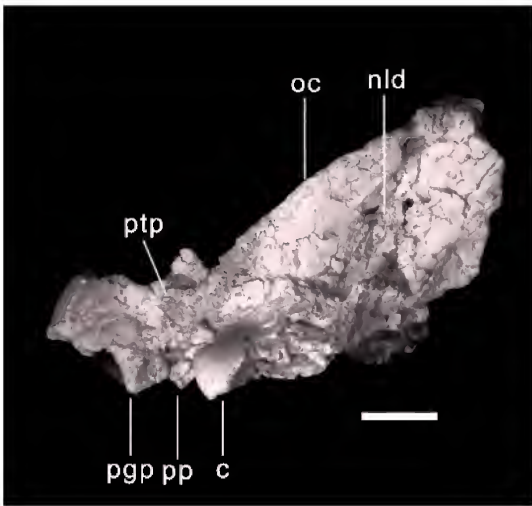

Fig. 5.   Ventral view of the right petrosal of *Litolophus gobiensis* (IVPP V16139). Abbreviations: **feo,** fenestra ovalis; **fr,** fenestra rotunda; **nf,** nutrient foramen; **pr,** promontorium; **smf,** stapedius muscles fossa; **tafc,** tympanic aperture of the facial canal. Scale = 5 mm.

Fig. 4.   Occipital view of the skull of *Litolophus gobiensis* (IVPP V16139). Abbreviation: **nld,** nuchal ligament depression; see legend for figure 2 for other abbreviations. Scale = 3 cm.
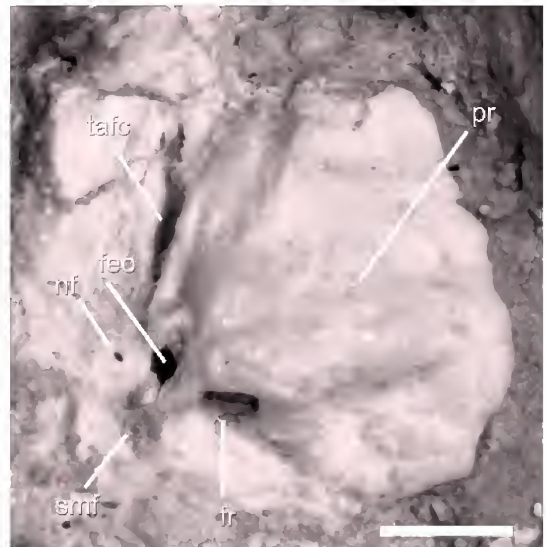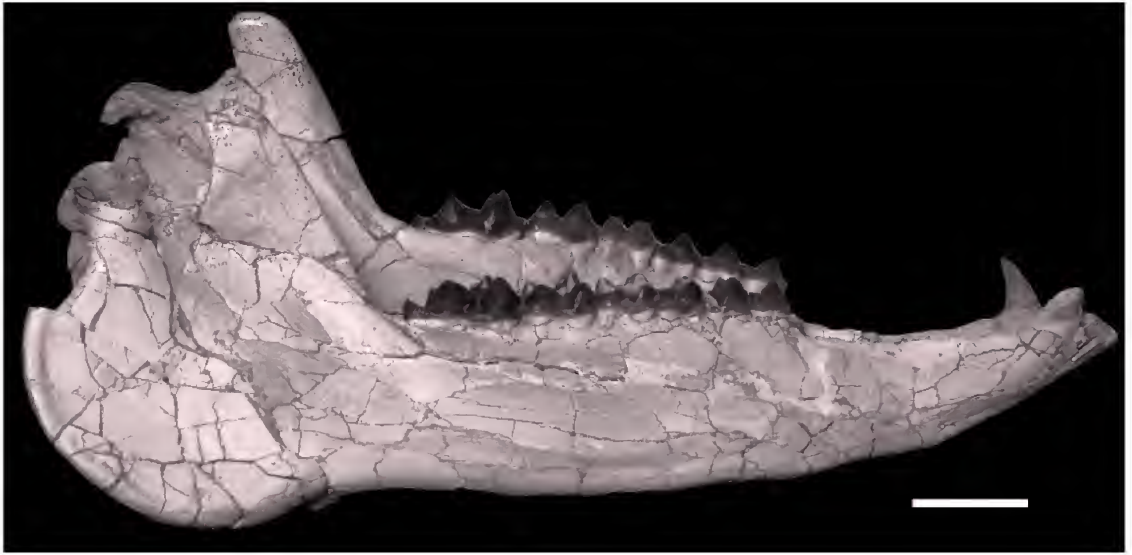
Fig. 6.   Right lateral view of the mandible of *Litolophus gobiensis* (IVPP V16149). Scale = 3 cm.

not enclose the external auditory meatus ventrally.

MANDIBLE: The mandibular symphysis is long and shallow, and its posterior border ends anterior to p2 by a short distance (fig. 6). On the anterior portion of the ventral surface of the mandibular body are a number of nutrient foramina. Three paired incisor alveoli are present, and i1 and i2 are almost equal in size, but i3 is much smaller. The canine is contiguous to i3, and is separated from p2 by a long diastema. The mental foramen is rather small and located below the posterior part of the diastema.

The mandibular spatium is narrow. The horizontal ramus is shallow and slender, with a slightly convex lower border. The mandibular angle is rounded, with a nearly semicircular border extending from the deep vessel notch to the condyle; the lateral surface of the mandibular angle is smooth and flat, while the medial surface is a little rough and concave around the margin. The masseteric fossa is a shallow triangular depression in the superior lateral region of the ascending ramus. The mandibular foramen is located posterior to m3, slightly lower than the alveolar border.

The coronoid process is higher than the condyle, and inclines posteriorly at the top. Although the condyle is situated relatively high above the occlusal line of the cheek teeth compared with that in *Eomoropus*, it is not raised to a great extent. The condyle extends laterally, with a flat doral surface and a rough posterior surface. The mandibular incision is broad, opening dorsoposteriorly.

UPPER   DENTITION: Three   procumbent pairs of upper incisors can be deduced from the alveoli (figs. 7A–D, 8, 9; appendix 1, 2). I2 is larger than I1, and I3 is the smallest. An isolated right premaxilla (V16143) preserves I3 and alveoli of I1 and I2. Several isolated upper incisors are also preserved, including a right I2 (V16144.1), two left I2s (V16144.2–3) and a right I3 (V16144.4).

I2 has a nearly semicircular crown, and the anterior and posterior ridges divide the crown into a convex buccal surface and a nearly flat lingual surface (fig. 7A, B). The crown is stouter than the root, and the latter slightly curves laterally. The cingulum is completely absent. Among the three known specimens of I2, two (V16144.2–3) are almost as high as long and have more rounded crowns than the third (V16144.1) which is slightly higher than long.

I3 is similar to I2 in morphology, but it is much smaller and its root curves more laterally (fig. 7C, D). The crown is slightly stouter than the anterior part of the root. V16143 has a rounded crown, nearly as high as long, while the other I3 (V16144.4) has a
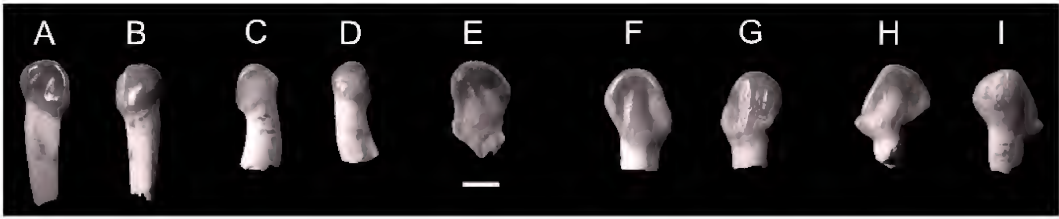
Fig. 7. Incisors of *Litolophus gobiensis*. **A–B**, lingual and buccal views of a left I2 (IVPP V16144.2); **C–D**, lingual and buccal views of a right I3 (V16144.4); **E**, lingual view of a left i1 (V16147); **F–G**, lingual and buccal views of a right i2 (V 16167.1); **H–I**, lingual and buccal views of a left i3 (V 16167.4). Scale = 5 mm.

nearly triangular crown, slightly higher than long. These subtly different morphologies between incisors may be just individual variation or related to sexual dimorphism.

The pointed upper canine is quite large and elliptical in cross section, with a prominent posterior ridge. The root is obviously stouter than the crown. The diastema between the canine and P1 is greater than that between the canine and I3 (fig. 2).

P1 is separated from the remaining cheek teeth by a diastema. It is single-cusped and longer than wide, with an elliptical outline and two roots. Two small cuspules are present, one each at the bases of the convex anterior and concave posterior ridges, and the posterior cuspule is more prominent than the anterior one. The cingulum is well developed at the posterolingual side of the tooth.

P2 of V16139 is roughly triangular in outline, longer than wide. The paracone is larger and higher than the metacone, and they are closely appressed. The groove between the paracone and the metacone is distinct on the lingual wall of the ectoloph, while that on the buccal wall is inconspicuous. The parastyle is small and low. The protocone is conical and

low, and posteriorly displaced. The short low metaloph extends from the protocone to the anterior base of the metacone. A small and low crest is present at the anterolingual base of the tooth, foreshadowing the development of the protoloph or the paraconule. The cingula are well developed at the anterior and posterior sides of the tooth, and the cingulum is also prominent at the posterobuccal side, while the lingual cingulum is absent. Although P2 of V16140-1 is basically similar to that of V16139, they are different in a number of features (fig. 9). For instance, the former is roughly trapezoidal in outline. The metacone is well developed with a distinguishable groove between the paracone and the metacone on the buccal side. The protocone is on the transverse axis of the tooth, from which the weak protoloph extends to the anterolingual base of the paracone. The metaloph is completely absent, so that a wide basin is present posterior to the protocone. The posterior cingulum is well developed. The protoloph and metaloph on P2 in some other specimens form a low loop.

P3 of V16139 is roughly quadrate in outline. Although the parastyle is small, it is more

Fig. 8. Occlusal view of upper cheek teeth of *Litolophus gobiensis* (IVPP V16139). Scale = 1 cm.
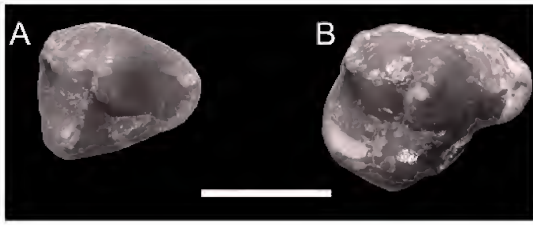
Fig. 9.   Occlusal view of right P2. **A,** IVPP V 16139; **B,** V 16140-1. Scale = 1cm.

prominent than that of P2. The paracone is slightly larger than the separate metacone, and they are almost equal in height on unworn teeth. The paracone rib is more prominent than the metacone rib, but in several other specimens the metacone rib is as distinct as the paracone rib. There is a shallow depression between the parastyle and the paracone rib on the buccal wall of the ectoloph. The protocone is on the transverse midline of the tooth, from which the metaloph extends labially to the anterolingual base of the metacone and the protoloph extends obliquely to the anterolingual base of the paracone. The metaloph is relatively strong and continuous, whereas there is usually a prominent paraconule on the protoloph as showed in figure 8. However, some specimens have relatively weak paraconules. P3 of V16142 has a rather weak and low protoloph, which joins the protocone at the base. The cingula are well developed at the anterior and posterior sides, prominent at the posterobuccal side, and faint to absent at the anterobuccal and lingual sides. The cingulum on V16140-1 is continuous at the buccal side and completely absent at the lingual side.

P4 is basically similar to P3, but it differs from P3 in having a rectangular outline that is wider than long, a more prominent parastyle, and a deeper depression between the parastyle and the paracone rib.

M1 is roughly quadrate in outline, slightly wider than long, and brachyodont. The parastyle is large and fan shaped with convex anterobuccal and flat posterolingual surfaces, and the depression between the parastyle and the paracone rib is deep. The paracone and metacone are separate and essentially vertical with the latter tilting slightly lingually. The paracone rib is well developed, while the buccal side of the metacone is nearly flat.

There is no mesostyle. The protocone is conical and posteriorly extended, and the protoloph, which is interrupted by the prominent paraconule, joins the ectoloph between the parastyle and the paracone. The hypocone is a bit higher than the protocone, extending the metaloph to the midpoint between the paracone and the metacone. Moreover, the most unusual character of the hypocone is that it is somewhat crescentic, with a very inconspicuous ridge extending posterobuccally from the top of the hypocone to the posterior cingulum. This situation can be identified by the presence of a slightly V-shaped worn surface on the hypocone in some specimens. The metaloph is high, oblique, relatively short, and uninterrupted. The anterior cingulum is slightly better developed than the posterior cingulum and the buccal cingulum is discontinuous in the middle, while the lingual cingulum is faint to absent, especially on the lingual sides of the protocone and the hypocone.

M2 is basically similar to M1, but it differs from M1 in being larger and having a larger and more buccally displaced parastyle. On unworn teeth, the paraconule, which is as high as the protocone and posteriorly convex, lies midway along the protoloph and divides the protoloph into buccal and lingual portions. The protoloph lingual to the paraconule is relatively deeply notched. The crescentic hypocone is more prominent than that on M1.

M3 is basically similar to M2, but differs from M2 in having a trapezoidal outline, a much larger and more buccally displaced parastyle, a more posteriorly displaced protocone, a short metacone with a flat top, posterobuccally rotated metacone, and a lophodont metaloph. Furthermore, the metaloph rotates posterobuccally, so that it is almost in line with the main part of the ectoloph. M3 of V16140-1 lacks the lingual cingulum. M3 of V16141-1 has an indistinct crista located posterolingual to the paracone as in *Butleria rusingensis* (Butler, 1965; de Bonis et al., 1995), and AMNH 26645 probably preserves the same crista according to the illustration (Colbert, 1934: fig. 2).

LOWER DENTITION: V16147 preserves a left i1, and V16148 preserves unerupted right and left i1 (figs. 7E–I, 10; appendix 1, 2). Several isolated lower incisors are also preserved,
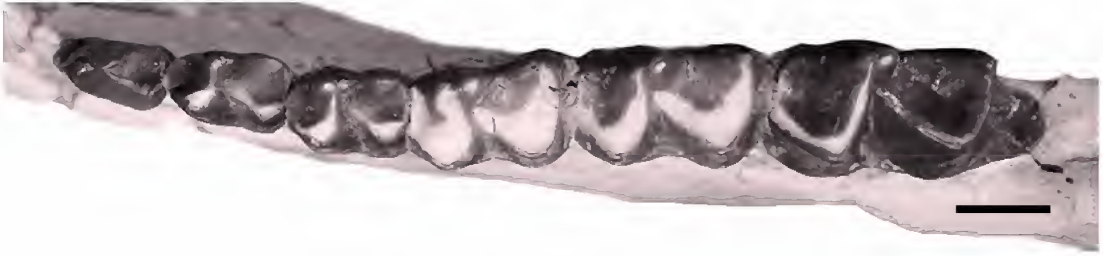
Fig. 10.   Occlusal view of lower cheek teeth of *Litolophus gobiensis* (IVPP V16149). Scale = 1 cm.

including three right i2s (V16167.1–3) and two left i3s (V16167.4–5). Incisor alveoli indicate that i1 and i2 are about equal in size, and both are much larger than i3, which is highly reduced.

The i1 has a roughly buccolingually compressed rectangular crown, rounded on top (fig. 7E). The anterior and posterior ridges divide the crown into a convex buccal surface and almost a flat lingual surface, and the latter is somewhat swollen at the base. The anterior ridge is shorter than the posterior ridge, on which a cuspule exists at the base. The tooth is symmetrical, so the posterior ridge is nearly parallel to the root. The crown is stouter than the root. No trace of a cingulid is present.

The i2 is similar to i1, but it is asymmetrical with an expanded area toward i1, so its posterior ridge is oblique medially (fig. 7F, G). The root is rounded in cross section. Furthermore, the lingual surface of V16167.1 has a strong ridge extending from the base to the top, with a concave margin, while the ridges are weak or nearly absent on the other two specimens of i2.

The i3 has a buccolingually compressed triangular crown, cusped on top, with a prominent cuspule at the base of the posterior ridge (fig. 7H, I). The tooth is asymmetrical as is i2, with a more expanded area toward i2, so its posterior ridge is more medially oblique. The lingual surface of i3 is similar to that of i2 except the crest extending from the base to the top is less developed. The crown is much stouter than the root, which is rounded in cross section. V16167.4 is a little higher and more cusped on top than V16167.5.

The lower canine is appressed to i3 and fairly large, with convex anterior and concave posterior ridges. The root is obviously stouter than the crown. The diastema between the canine and p2 is considerably long.

The p1 is absent. The p2 is laterally compressed with two roots, having a single-cusped crown and an elliptical outline. The anterior ridge is steep and slightly convex, terminating in a small cuspule at the base. The posterior ridge is long and slightly concave, forming a rudimentary talonid basin at the base, which is bounded by the cingulumlike ridge posteriorly. On some specimens there is a third ridge extending posterolingually downward from the main cusp to the base. A weak cingulid is present anteriorly, but buccal and lingual cingulids are absent.

The p3 is rectangular in outline, longer than wide. The trigonid basin is higher, longer, and narrower than the talonid basin. The protoconid sends the protolophid anteriorly, terminating low at the short and weak paralophid. The metalophid is strong and oblique, having a shallow notch midway. The metaconid is conical, to which a faint "metastylid" is present posteriorly on some specimens. The hypoconid is low and prominent, sending the cristid obliqua anterolingually. The cristid obliqua is upward raised, joining the back of the trigonid slightly below the notch of the metalophid. The entoconid is indistinct, and the hypolophid is weak and cingulumlike. The anterior and buccal cingulids are weak, but usually prominent in the ectoflexid. The posterior and lingual cingulids are absent.

The p4 is similar to p3, but differs from p3 in being wider, and in having a nearly transversely extended metalophid, rudimentary "metastylid," more lingually inclined cristid obliqua, and more prominent entoconid and talonid basin. Furthermore, the p4 trigonid is about the same length as the talonid.

The unworn m1 is composed of two crescents, the anterior U-shaped and the posterior V-shaped crescents. Heavily worn

teeth, however, consist of two V-shaped crescents. The trigonid basin is shorter, slightly narrower and higher than the talonid basin. The protolophid extends anterolingually, then turns lingually at the base forming the short paralophid. The paraconid is distinct and a little lower than the metaconid, and the paralophid is relatively high, so the trigonid basin is not very deep. The metalophid is well developed and nearly transversely extended, with the protoconid almost in line with the metaconid. In unworn teeth there are wide notches on the metalophids. The "metastylid" is prominent, and slightly smaller and lower than the metaconid. The cristid obliqua is lingually directed, extending from the hypoconid to the buccal side of the "metastylid" in a relatively high position. The hypolophid is oblique and widely notched, with the hypoconid slightly anterior to the entoconid. The metaconid is the highest cusp on the molar, and the "metastylid" is as high as the entoconid, both of which seem slightly higher than the protoconid and the hypoconid. The buccal part of m1 is more rapidly worn down than the lingual part. The cingulids are similar to those of p4, but the posterior cingulid is prominent and its lingual portion is raised upward without a cuspule.

The m2 is basically similar to m1, but it differs from m1 in its larger size, less prominent paraconid and deeper trigonid, more separate "metastylid" from the metaconid, and slightly better developed posterior cingulid.

The m3 differs from m1 and m2 in having a hypoconulid lobe much lower than the talonid, trigonid basin wider than the talonid basin, lightly oblique metalophid, and more prominent and separated "metastylid." Furthermore, the hypoconulid lobes have variable sizes and outlines in different specimens. The hypoconulid lobes in some specimens are relatively small, having smooth surfaces and triangular outlines, while others are large, having relatively rough surfaces and semicircular outlines. The buccal edge of the hypoconulid lobe is lower than the lingual one, which runs parallel to a weak to faint crest extending anteroposteriorly on the surface of the hypoconulid lobe. In most specimens m3 preserves a small entoconulid on the lingual base of the talonid basin.

COMPARISONS AND DISCUSSION

The new materials are unquestionably from *Litolophus gobiensis*, but display some variations in comparison with the holotype, such as various positions of P2 protocone, and presence of a considerable longer diastema between the canine and P1 than that between P1 and P2. Radinsky (1964a) and Lucas and Schoch (1989) made detailed dental comparisons between *Litolophus* and other Eocene chalicotheres. These authors thought that *Litolophus* differs from *Eomoropus* in lacking mesostyles on upper molars, and in having a larger size, a diastema between P1 and P2, a relatively smaller and more posteriorly displaced protocone on P2, more convex and slightly less lingually depressed paracones on M1–2, the metacone and metaloph posterobuccally rotated on M3, more posteriorly extended protocones on M1–3, differentiated p2 talonid, slightly more oblique p3–m3 cristid obliqua, and shorter premolar series relative to molar series. However, the new materials reveal that P2 protocones vary in position from posterior to medial and the cristid obliqua of p3–m3 is more lingually oblique than that of *E. amarorum*, but the differences are not obvious between *Litolophus* and Asian *Eomoropus*. Moreover, new materials also add some important characters that distinguish *Litolophus* from *Eomoropus*. For instance, *Litolophus* is different from *Eomoropus* in that the P2–4 metalophs in *L. gobiensis* join the base of the ectolophs, namely at the anterolingual base of the metacones, whereas the P2–4 metalophs in most *Eomoropus* except *E. pwanyunti* connect rather high on the ectolophs, in some cases to the top of the metacones (Peterson, 1919; Zdansky, 1930; Remy et al., 2005). *L. gobiensis* is also different from *Eomoropus* in having the P2 metaloph weak to absent, P3–4 paraconules usually well developed, the metacones on molars nearly vertical and much less lingually tilted, p3 paraconid less prominent, m1 paraconid more prominent and higher, m1–2 posterior cingulids raised upward without cuspate hypoconulids, and m3 with better developed hypoconulid lobe. The metalophs of *Litolophus gobiensis*, as well as *E. minimus*, are more oblique and relatively shorter than the protolophs, while those of *E. amarorum*,
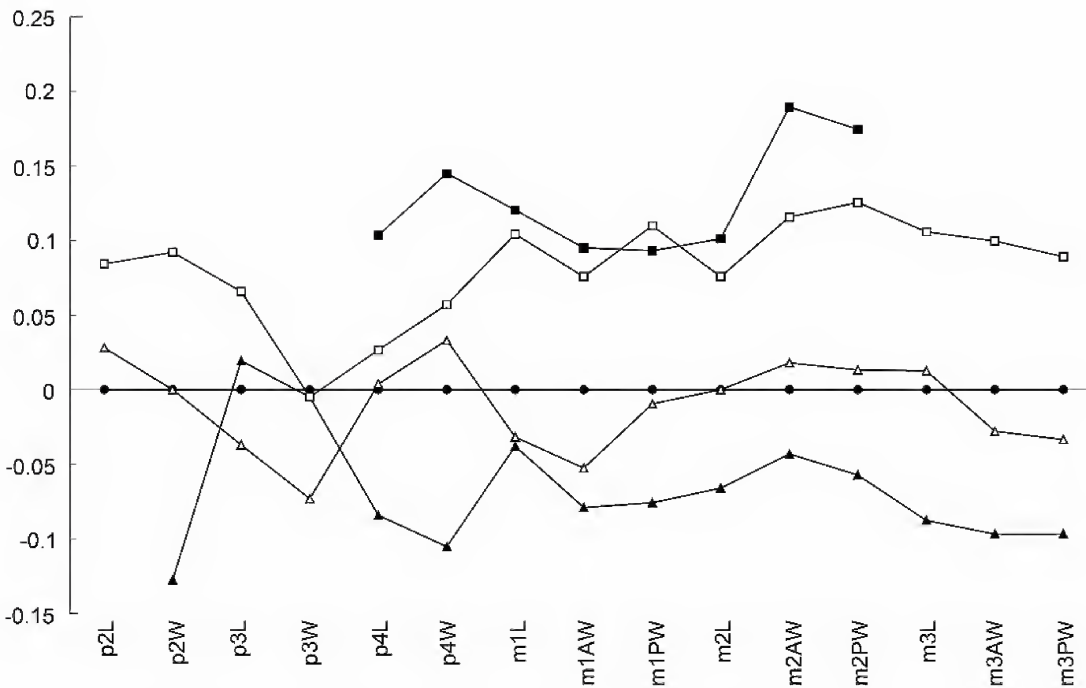
Fig. 11. Log-ratio diagram comparing the mean value of lower teeth dimensions of *Litolophus gobiensis* (V16149, V16150) (open squares), *Grangeria canina* (filled squares), *Eomoropus amarorum* (filled circles; as standard), *G. anarsius* (open triangles), and *E. quadridentatus* (filled triangles). Data sources from Lucas and Shoch (1989, table 23.2) (L, length; AW, trigonid width; PW, talonid width).

E. quadridentatus, and *E. pawnyunti* are less oblique and almost as long as the protolophs. Moreover, from the log-ratio diagram of the lower teeth (fig. 11), *L. gobiensis* is clearly larger than *E. amarorum*, and *E. quadridentatus* is even smaller than *E. amarorum*. The specimen (SDM 84006) originally assigned to *E. quadridentatus* from Qufu, Shandong Province, China, probably represents a new species of *Eomoropus*, mostly because SDM 84006 has more oblique metalophs and nearly anteroposteriorly compressed parastyles on the upper molars (Shi, 1989; Bai, 2008).

Only *E. amarorum* (AMNH 5096) preserves parts of the skull in *Eomoropus* (Cope, 1884; Osborn, 1913; Radinsky, 1964a), but the zygomatic arches and preorbital portions of the specimen are not preserved. The skull of *L. gobiensis* differs from that of *E. amarorum* in the following characters: (1) The parietal crests gradually converge at the sagittal crest, whereas the parietal crests in *E. amarorum* are nearly transverse, extending from the postorbital processes and then converging gradually

toward the sagittal crest. (2) *L. gobiensis*, with a small orbit, lacks the supraorbital foramen, while *E. amarorum* has a large round orbit and a supraorbital foramen. (3) The shape of the occipital surface in *L. gobiensis* is triangular, and the occipital crest extends ventrally to join the temporal crest. In contrast, the shape of the occipital surface in *E. amarorum* is roughly rectangular, and the occipital crest contracts ventrally. (4) The paroccipital process on *L. gobiensis* is slender and short, with a flat anterior surface and a longitudinally concave and latitudinally convex posterior surface, and is completely separated from the relatively broader and larger posttympanic process. On the other hand, *E. amarorum* has a large and stout paroccipital process that is separated from a relatively short posttympanic process only by an incision. *L. gobiensis* and *E. amarorum* share some similar characters. Both have long and sharp sagittal crests, stout postglenoid processes, and occipitals overhanging the condyles to certain degree. The mandible of *L. gobiensis* differs from that of *E.*

amarorum in having a higher condyle and a round mandibular angle projecting more ventrally but less posteriorly.

Zdansky (1930) erected a new species *Eomoropus*? *major* based on an isolated M2? (PMUM 3453), but Radinsky (1964a) thought it probably belonged to *Grangeria*? *major*. Lucas and Schoch (1989) further identified the specimen as M1 of *G. canina*. Careful comparison shows that PMUM 3453 is more similar to *Eomoropus* than to *Grangeria* (Bai, 2008). If so, *E. major* should be considered as a valid species, and the upper molars of *G. canina* remain unknown.

Compared with *Grangeria*, *Litolophus* is distinct in the following characters: (1) The p4 dimensions of *L. gobiensis* (fig. 11) are close to those of *G. anarsius*, but its lower molar dimensions, especially m1, which is the least variable in size in mammals (Gingerich, 1974), are closer to those of *G. canina* than to other species. However, *L. gobiensis* is slightly smaller than *G. canina*, and both are larger than *G. anarsius*; the latter is more comparable with *E. amarorum*. (2) The lower canine of *L. gobiensis* is much smaller than that of *Grangeria*. (3) The diastema between P1 and P2 in *L. gobiensis* is longer than that of *G. canina*. (4) The P2 protoloph in *L. gobiensis* is absent or less developed than that in *G. canina*. (5) *L. gobiensis* lacks mesostyles but has buccally projected parastyles and more prominent paracone ribs on upper molars. In contrast, *G. anarsius* has small mesostyles, more buccally projected parastyles, and less prominent paracone ribs. (6) *L. gobiensis* has more posteriorly extended protocones and more oblique metalophs on upper molars. (7) The M1–2 metacones in *L. gobiensis* are less lingually tilted than those on *G. anarsius*.

Similarities in premolar cusp patterns and lower cheek teeth between *L. gobiensis* and *G. canina* were mentioned by Radinsky (1964a). *L. gobiensis* is similar to *G. canina* in having a relatively large size, a diastema between P1 and P2, metalophs joining the ectoloph in a low position on P3, the paraconule present on P3, oblique cristid obliqua on lower molars, and upward raised posterior cingulids without a cuspate hypoconulid on m1–2. Furthermore, the manus and pes of *L. gobiensis* are similar to those of *G. canina* (Lucas and Schoch,

1989), suggesting a close phylogenetic relationship between them.

The holotype of *G. anarsius* (USNM 21097) includes most of the left side of the skull and the left lower jaw (Gazin, 1956). It differs from *L. gobiensis* in the following features: (1) *L. gobiensis* is dolichocephalic, with a long and relatively low skull, whereas *G. anarsius* is brachycephalic, with a relatively short and high skull. (2) *L. gobiensis* has a small orbit above M3, and the paroccipital process is separate from the posttympanic process. *G. anarsius* is similar to *E. amarorum* in having a large and round orbit above M2 and M3, and the paroccipital process is close to the posttympanic process. (3) The depth below the lower margin of the orbit in *G. anarsius* is relatively greater than that in *L. gobiensis*. (4) The mandible of *L. gobiensis* is relatively long and slender, whereas that of *G. anarsius* is relatively robust.

Pappomoropus taishanensis is an Early Eocene chalicothere from the Wutu Formation, Wutu Basin, Shandong Province (Tong and Wang, 2006). *L. gobiensis* differs from *P. taishanensis* in lacking p1, and in having p2 with a less prominent paraconid and a more inclined cristid obliqua on lower molars (Tong and Wang, 2006). Furthermore, *L. gobiensis* has a larger body size, an inconspicuous paraconid on p3, more prominent entoconids on p3–p4, a cristid obliqua extending upward to the posterior wall of the metalophid on p3–m2, and a U-shaped trigonid basin on lower molars. On the other hand, *P. taishanensis* has a smaller size, p3 with the prominent paraconid, rudimentary to small entoconids on p3–p4, a cristid obliqua extending slightly downward to the posterior wall of the metalophid on p3–m2, and a roughly quadrangular trigonid basin on the lower molars. Compared with m3 of *L. gobiensis*, that of *P. taishanensis* has a weak cristid obliqua extending to the base of the posterior wall of the metalophid, and an almost isolated hypoconid and entoconid separated by a deep notch.

The Bumbanian *Protomoropus gabuniai* from Naran Bulak Formation, Naran Bulak area, Mongolia, is based on the holotype and a paratype originally identified as "*Hyracotherium*" *gabuniai*, specimens originally referred to *Homogalax namadicus*, and new material of a maxilla with P4–M3 (Hooker

and Dashzeveg, 2004). However, the same new material was also assigned to *Homogalax namadicus* by other authors (Lucas and Kondrashov, 2004). We follow Hooker and Dashzeveg (2004) regarding the identification of those specimens. As observed by Hooker and Dashzeveg (2004), *Litolophus* differs from *Protomoropus* in having "a more mesial position of the ectoloph attachment of the metaloph, posteriorly extended protocone on the molars, more closely approximated paracone and metacone on P4, and autapomorphic elongation of the molars and reduction in size of the premolars." Of the lower molars, *Litolophus* has a high cristid obliqua joining the "metastylid," a more oblique protolophid, indistinguishable hypoconulids on m1–2, and a much smaller and lower hypoconulid lobe on m3 as recognized by Hooker and Dashzeveg (2004). Furthermore, *Litolophus* is larger than *Protomoropus* and has a low connection between the metaloph and the ectoloph on P4, a paraconule on P4, more prominent paracone ribs and paraconules on molars, interrupted lingual cingula on upper molars, less developed buccal cingulids on lower molars, more prominent "metastylids," and no metastyles on M3.

Litolophus shares some similarities with *Lophiaspis* and *Paleomoropus* (Radinsky, 1964a; Hooker and Dashzeveg, 2004). They all lack mesostyles on upper molars. The Neustrian *Lophiaspis maurettei*, found near Palette, Aix-en-Provence, France, has been placed either in the Lophiodontidae by some authors (Fischer, 1977; Prothero and Schoch, 1989; Schoch, 1989) or in the Chalicotherioidea by others (Radinsky, 1964a; Hooker, 1989). *Litolophus* differs from *Lophiaspis* in having larger and relatively longer upper molars, more lingually depressed paracones, more posteriorly extended protocones, and posterobuccally rotated M3 metaloph and metacone (Radinsky, 1964a). Moreover, *Litolophus* is distinguished from *Lophiaspis* by having a prominent paraconule and metaloph on P3, a prominent paraconule on P4, less lingual tilt of the metacones on M1–2, more posteriorly extended paraconules on upper molars, relatively continuous buccal cingulum, straight and high cristid obliqua which is more lingually directed, and a larger hypoconulid lobe on m3

(Savage et al., 1966; Hooker and Dashzeveg, 2004).

The middle Wasatchian *Paleomoropus*, from the Clarks Fork Basin, Wyoming (Radinsky, 1964a; Gingerich, 1991), preserves only three upper molars. It has been placed in the Eomoropidae (Radinsky, 1964a) or in the Lophiodontidae (Fischer, 1977; Hooker and Dashzeveg, 2004). *Litolophus* differs from *Paleomoropus* in being larger and relatively longer, and having better developed paraconules and parastyles, more acute lophs, oblique and relatively short transverse lophs, more anterior position of the connection between the ectoloph and the metaloph, less lingually displaced and tilted metacones on M1–2, more posteriorly extended protocones, more prominent paracone ribs, a posterobuccally rotated M3 metaloph and metacone, and interrupted lingual cingula.

PHYLOGENETIC ANALYSIS

Previous Work: According to McKenna and Bell (1997), Eocene chalicotheres placed in the Eomoropidae historically consist of seven genera, including *Eomoropus*, *Grangeria*, *Litolophus*, *Paleomoropus*, *Lophiaspis*, *Lunania*, and *Danjiangia*. This group is considered paraphyletic and its members give rise to post-Eocene Chalicotheriidae (sensu Coombs, 1989, 1998). *Protomoropus* and *Pappomoropus* from Mongolia and China were regarded as basal chalicotheres (Hooker and Dashzeveg, 2004; Tong and Wang, 2006). The phylogenetic status of *Lunania* and *Danjiangia* are equivocal. *Lunania* may represent either a diminutive chalicothere or a phenacolophid (Chow, 1957, 1962; Lucas and Schoch, 1989; Huang, 2002), whereas *Danjiangia* is assigned to either a primitive chalicothere or a brontothere (Wang, 1995; Hooker and Dashzeveg, 2003, 2004). Phylogenetic resolution of these early forms depends on discovery of better-preserved specimens as well as more thorough phylogenetic analyses including more taxa of both chalicotheres and brontotheres. Our analysis does not include *Lunania* and *Danjiangia*. *Paleomoropus* and *Lophiaspis* represent either a lophiodont or a chalicothere as discussed above. Radinsky (1964a) suggested that by the late Eocene chalicotheres had radiated into at least

three lineages: *Litolophus* represents a persistently primitive stock, *Eomoropus* is a representative of the main line of chalicotherioid evolution, and *Grangeria* represents a specialized offshoot from *Eomoropus*. Coombs (1989, 1998) also considered *Litolophus* as the stem taxon, but the relationships between *Eomoropus* and *Grangeria* were unresolved. Furthermore, the phylogenetic analysis by Hooker (1989) placed Lophiodontidae as the sister group to Chalicotherioidea (sensu Radinsky, 1964a) and nested in the clade Ancylopoda (Hooker, 1989; Froehlich, 1999). However, explicit phylogenetic relationships among typical Eocene chalicotheres, including *Eomoropus*, *Grangeria*, and *Litolophus*, are still poorly known. Here we perform a phylogenetic analysis using only the cranial and dental characters.

TAXA AND CHARACTERS: The analyses were based on a matrix of 21 OTUs (operational taxonomic units) and 58 characters (appendix 4). We use OTU instead of taxa because the specimens SDM 84006 is included in the analyses. Of the 58 characters, 46 are dental (29 upper and 17 lower teeth), 7 cranial, and 5 mandibular. Among these characters, 19 characters and their states were used by Wang (1995), Holbrook (1999), Hooker and Dashzeveg (2004) and Anquetin et al. (2007), 9 characters are modified from previous work, and 30 characters are new. The Early Eocene genera *Cardiolophus* and *Homogalax wutuensis* were chosen as outgroups because *Homogalax wutuensis* has been regarded as the sister taxon to Chalicotherioidea (sensu Hooker and Dashzeveg, 2004), which is comprised of Lophiodontidae and Chalicotheriidae, and *Cardiolophus* is the sister taxon to the *Homogalax wutuensis*–Chalicotherioidea clade. The primitive rhinocerotoid *Hyrachyus* and tapiroid *Heptodon* were included in the analysis in order to test the phylogenetic status of *Lophiodon*. In the following paragraphs we briefly comment on some new or modified characters used in the analyses. The complete list of characters is in appendix 3 and the data matrix is in appendix 4. Upper teeth characters of *Schizotherium avitum* are based on *Schizotherium* cf. *S. avitum* (AMNH 26061) (Coombs, 1978b). *Eomoropus minimus* is based on specimen V 9911 (Zong et al., 1996).

Character 2. Post P1 diastema: (0) present, (1) absent. This corresponds to character 52 of Hooker and Dashzeveg (2004), but the character states are different. The length of the post P1 diastema relative to that of postcanine diastema is not applicable, because most taxa do not preserve canines.

Character 6. P3 paraconule: (0) absent, (1) present. This corresponds to character 3 of Wang (1995). A notch between the protoloph and the protocone on P3 in *G. canina* implies the development of a paraconule, which is similar to some cases in *Litolophus*.

Character 9. P3 metaloph: (0) absent, (1) weak, not joining the ectoloph or the protocone, (2) lophid, joining the ectoloph in a low position, (3) lophid, joining the ectoloph in a high position. Ordered. This corresponds to character 4 of Wang (1995), but the character states are different. State 2 (lophid, joining the ectoloph) of Wang's (1995) character 4 we have split into two character states, showing the different joining positions between the ectoloph and the metaloph. Similar character states are applied to character 12.

Character 15. Upper molar parastyle: (0) separated from the ectoloph, (1) fused together with the ectoloph. New character. Radinsky (1964a) indicated that fusion of the parastyle with the ectoloph in post-Eocene chalicotheres is a derived character, while most Eocene chalicotheres have the separated parastyles from ectolophs.

Character 16. M3 parastyle extends: (0) buccally, (1) strongly buccally, (2) anterobuccally. New character. Unordered. This is similar to character 14 of Wang (1995), but the character and character states are different. If the orientation of the crest between the parastyle and the ectoloph is nearly transverse, the M3 parastyle is strongly buccally extended. However, in *Hyrachyus* and *Heptodon* the parastyles are closely appressed to the ectoloph anterobuccally.

Character 17. Upper molar protocone: (0) does not extend posteriorly, (1) extends posteriorly, (2) strongly extends posteriorly. New character. Ordered. The upper molar protocone of *Moropus* lies barely in the anterior half of the tooth, representative of strongly posteriorly extended character state.

Character 24. Upper molar paracone: (0) vertical, (1) tilted buccally slightly, (2) markedly tilted buccally, (3) tilted lingually. Unordered. This corresponds to character 45 of Hooker and Dashzeveg (2004), but the character states are different. Although the paracones of *Eomoropus*, *Grangeria*, and post-Eocene chalicotheres tilt lingually to different extents, they possess lingually tilted rather than vertically implanted paracones on upper molars.

Character 45. Lower molar "metastylid": (0) larger than or equal to metaconid, (1) smaller than metaconid, (2) absent. Ordered. This corresponds to character 40 of Hooker and Dashzeveg (2004), but the character states are different. Some taxa such as *Lophiodon*, *Hyrachyus*, and *Heptodon* lack "metastylids" on lower molars.

Character 57. Condyle position: (0) low, (1) high. New character. If the condyle is slightly above the occlusal surface, the condyle position is low, whereas if the condyle is much higher above the occlusal surface, the condyle position is high.

RESULTS: The matrix was analyzed using PAUP 4.0b10 (Swofford, 2001) with the branch and bound algorithm. A total of 48 equally most parsimonious trees (MPTs) of 178 steps were identified. The consistency index (CI) for each tree is 0.4775, the consistency index excluding uninformative characters is 0.4624, and retention index (RI) is 0.5991. The strict component and 50% majority rule consensus trees are presented in figure 12 and figure 13, respectively.

Although the phylogeny of Eocene chalicotheres is not well solved in the strict component consensus tree, the cladogram shows some interesting results (fig. 12). First, *Moropus* and *Ansiodon*, representing Schizotheriinae and Chalicotheriinae respectively, form a clade, and *Schizotherium* is the sister group to the *Moropus-Ansiodon* clade. The result indicates that "Schizotheriinae" is probably a paraphyletic group. Second, SDM 84006, originally assigned to *E. quadridentatus* (Shi, 1989), is the sister taxon to the *Schizotherium-Moropus-Ansiodon* clade. The result supports the idea that SDM 84006 is different from any other *Eomoropus* species and probably represents a new advanced form

(Bai, 2008). Third, *E. ulterior* (VM 0053) and *E. amarorum* form a clade, which is characterized by absence of a p3 entoconid (character 33) and lower molar "metastylid" equal to the metaconid in size (character 45). This result supports the original identification and comparison that assigned the specimen to *Eomoropus ulterior* and reveals a close relationship between VM 0053 and *E. amarorum* (Chow, 1962). However, the result contradicts Radinsky's assignment of VM 0053 to *Litolophus? ulterior* (Radinsky, 1964a), which was based on a relatively shorter premolar series and slightly more oblique molar cristid obiquas. It is more convincing to assign VM 0053 to *Eomoropus* given its Sharamurunian age (Tong et al., 1995; Wang et al., 2007) in which species of *Eomoropus* dominated among chalicotheres. The Arshantan *L. gobiensis* is much older. Morphologically, *E. ulterior* is smaller than *L. gobiensis* and has a more prominent paraconid on p3, no entoconids on p3-4, a much shorter and slightly narrower trigonid base in relation to the talonid base, and small cuspidate hypoconulids on m1–2. Finally, *Lophiodon* is the sister taxon to the *Hyrachyus-Heptodon* clade, supporting the analysis of Holbrook (2009). Chalicotherioidea (sensu Radinsky, 1964a) is monophyletic if *Lophiodon*, even Lophiodontidae, is excluded from Ancylopoda (sensu Hooker, 1989), and Lophiodontidae is not a sister group to Chalicotherioidea (sensu Radinsky, 1964a).

The phylogeny of Eocene chalicotheres is not solved in the strict component consensus tree, but is well solved in the 50% majority rule consensus tree. The 50% majority rule consensus tree (fig. 13) shows that two post–earliest Eocene chalicothere lineages (node 31) are present. The first lineage represents the main clade of chalicotheres, including "*Grangeria*" *anarsius*, *Eomoropus*, and post-Eocene chalicotheres. The second clade, consisting of *Litolophus gobiensis* and *Grangeria canina*, is the sister group and stem member to the main clade. According to the cladogram, "*Grangeria*" *anarsius*, originally referred to *Eomoropus*, is the sister taxon to the *Eomoropus-Schizotherium-Moropus-Ansiodon* clade. Radinsky (1964a) transferred the species from *Eomoropus* to *Grangeria* mainly based on the enlarged canine and deep mandible. In contrast, our analysis indicates that the enlarged canine
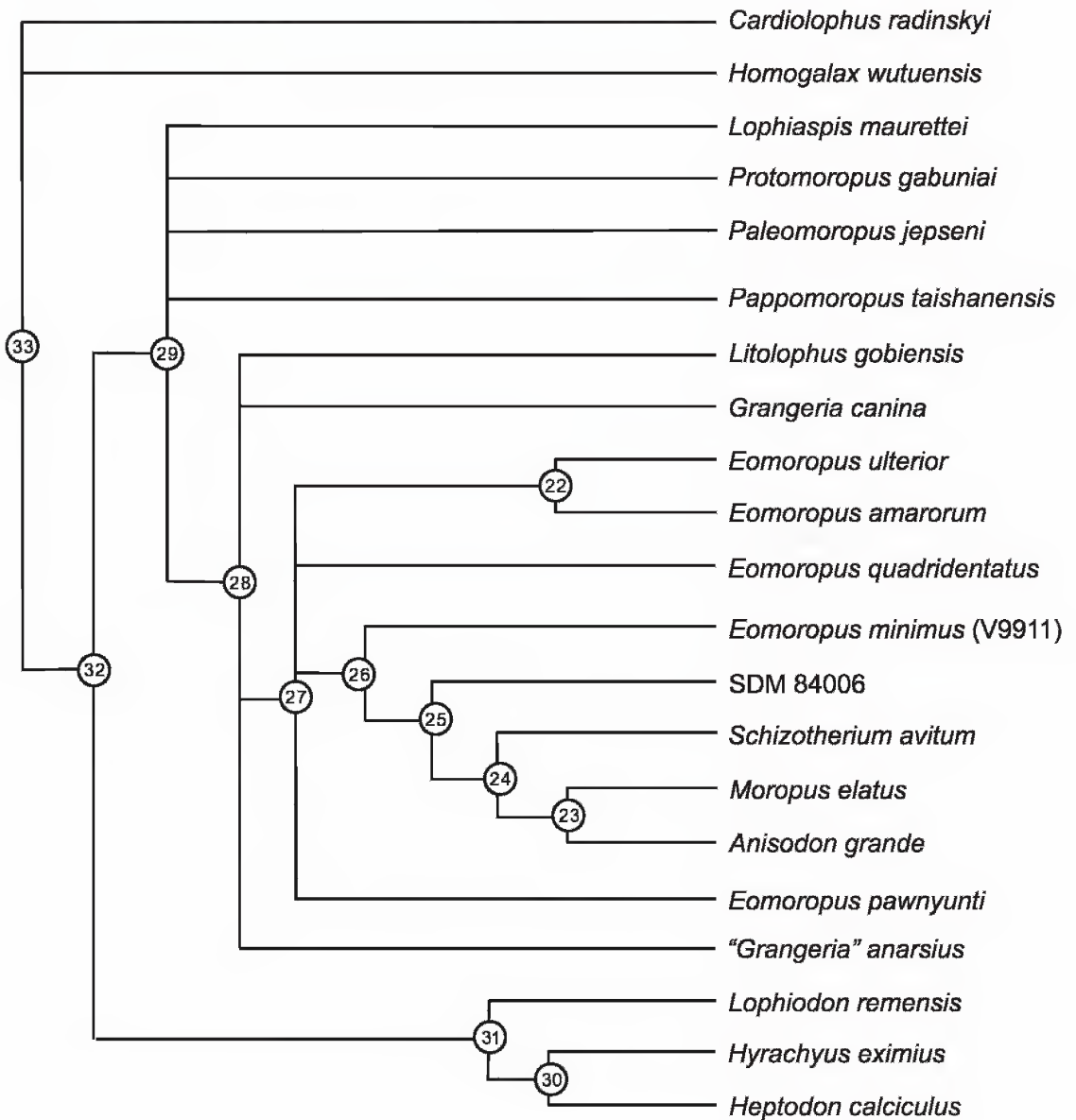
Fig. 12. Strict component consensus of 48 equally most parsimonious trees.

(character 46) and deep mandible (character 58) are characters resulting from parallelism. Based on our analyses, it is probably better to consider "*Grangeria*" *anarsius* a species of *Eomoropus*, as originally identified. Moreover, the phylogenetic analysis indicates that the genus *Eomoropus* may not be a monophyletic group, which should be further tested by including more advanced taxa in the phylogenetic analysis in the future. In addition, *Lophiaspis* rather than *Lophiodon* is the sister taxon to node 31 (fig. 13). This differs from the *Lophiaspis-Lophiodon* pairing in a previous analysis (Hooker and Dashzeveg, 2004). *Paleomoropus*, *Pappomoropus*, and all other chalicotheres except *Protomoropus* form an unresolved trichotomy. *Protomoropus* is the stem taxon to all other chalicotheres.

Fig. 13.   Majority rule (50%) consensus of 48 equally most parsimonious trees.

In order to solve the phylogenetic relationships at node 27, 28, and 29 in the strict component consensus tree, we use the strict reduced consensus (SRC) method (Wilkinson, 1994, 1995, 2003). The RadCon (Thorley and P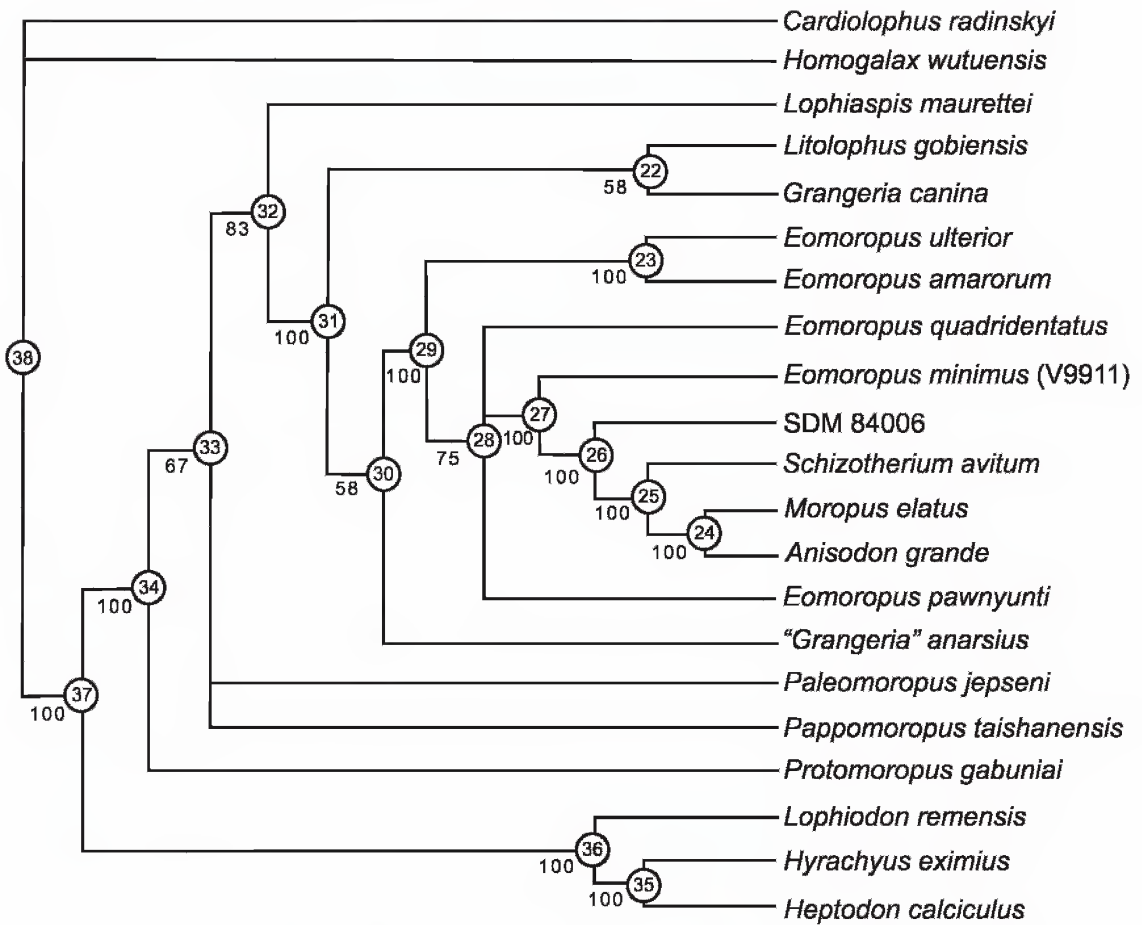age, 2000) produces the SRC profile consisting of four trees. The derivative SRC tree, which is constructed by fusing basic SRC trees, probably provide more informative relationships than does any single SRC tree (Wilkinson, 1995). As suggested by Mihlbachler (2008), the derivative SRC tree could be reconstructed by using "PAUP to prune all taxa (a posteriori) from the primary trees already pruned by SRC and then computing a strict consensus." Figure 14 presents the derivative SRC tree, which prunes unstable *Pappomoropus taishanensis*, *Grangeria canina*, and *Eomoropus pawnyunti*. The clado-gram shows that *Litolophus gobiensis* is the sister group to the post–Early Eocene chalicothere (node 29), and *Paleomoropus jepseni* is the sister group to the other chalicotheres except *Protomoropus gabuniai*. The result indicates that *Litolophus gobiensis* is more derived than other Early Eocene chalicotheres that lack mesostyles on upper molars, and it is also the least derived compared with post–Early Eocene chalicotheres which have mesostyles. The result is also consistent with some topologies in the 50% majority rule consensus. For instance, *Lophiaspis*, instead of *Lophiodon*, is the sister taxon to node 30; "*G.*" *anarsius* is the sister group to node 28, representing a relatively primitive position in post–Early Eocene chalicotheres. Moreover, from the log-ratio diagram (fig. 11) and derivative SRC tree (fig. 14), the
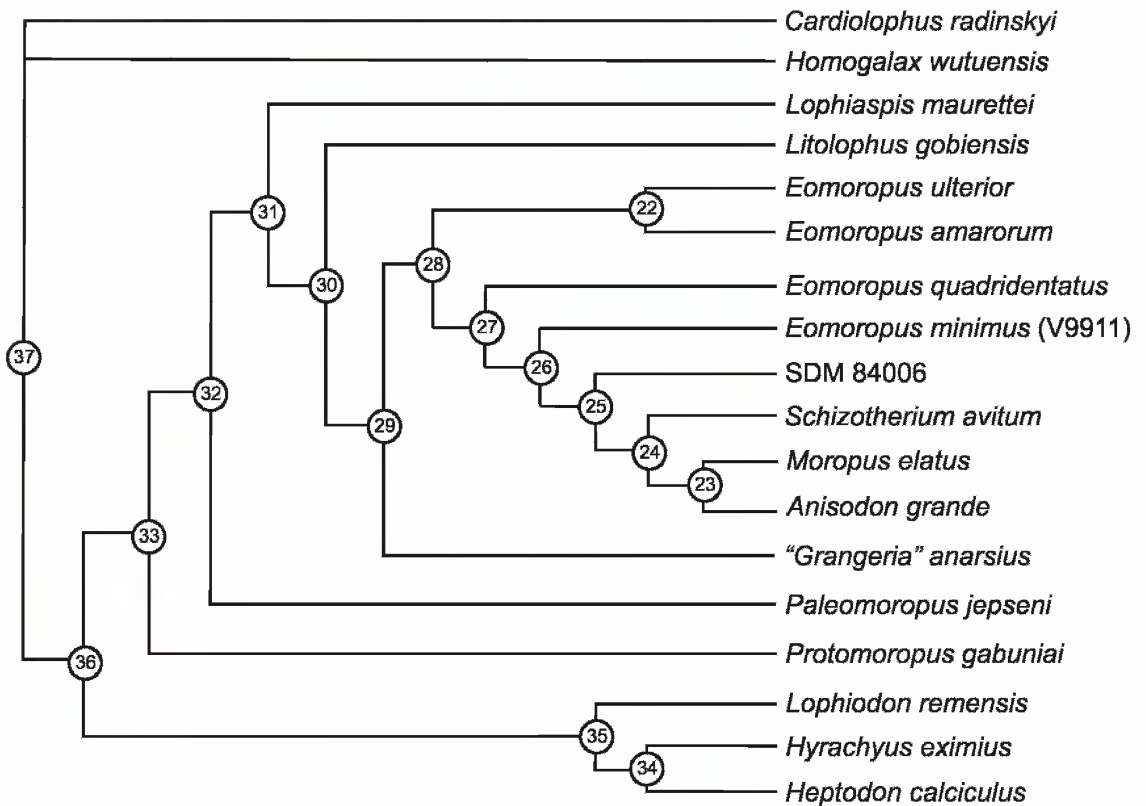
Fig. 14.   The derivative strict reduced consensus (SRC) tree constructed by fusing four SRC trees.

post–Early Eocene chalicotheres from primitive *"G." anarsius* to advanced *E. minimus* appears to decrease their body sizes, whereas from *E. minimus* to relatively advanced forms the body sizes have increased (figs. 11, 14).

ACKNOWLEDGMENTS

REFERENCES

Anquetin, J., P.O. Antoine, and P. Tassy. 2007. Middle Miocene Chalicotheriinae (Mammalia, Perissodactyla) from France, with a discussion on chalicotheriine phylogeny. Zoological Journal of the Linnean Society 151: 577–608.

Bai, B. 2006. New materials of Eocene Dinocerata (Mammalia) from the Erlian Basin, Nei Mongol (Inner Mongolia). Vertebrata PalAsiatica 44: 250–261.

Bai, B. 2008. A review on Chinese Eocene chalicotheres *Eomoropus* and *Grangeria*. *In* W. Dong (editor), Proceeding of the 11th Annual Meeting of the Chinese Society of Vertebrate Paleontology: 19–30. Beijing: China Ocean Press.

de Bonis, L., G. Bouvrain, G. Koufos, and P. Tassy. 1995. Un crâne de chalicothère (Mammalia, Perissodactyla) du Miocène supérieur de Macédoine (Grèce): remarques sur la phylogénie des Chalicotheriinae. Palaeovertebrata 24: 135–176.

Bulter, P.M. 1965. Fossil mammals of Africa No. 18: East African Miocene and Pleistocene chalicotheres. Bulletin of the British Museum (Natural History) 10: 163–237.

Chow, M.-Z. 1957. On some Eocene and Oligocene mammals from Kwangsi and Yunnan. Vertebrata PalAsiatica 1: 201–214.

Chow, M.-Z. 1962. A new species of primitive Chalicothere from the Tertiary of Lunan, Yunnan. Vertebrata PalAsiatica 6: 219–224.

Colbert, E.H. 1934. Chalicotheres from Mongolia and China in the American Museum. Bulletin of the American Museum of Natural History 67(8): 353–387.

Coombs, M.C. 1978a. Reevaluation of early Miocene North American *Moropus* (Perissodactyla, Chalicotheriidae, Schizotheriinae). Bulletin of Carnegie Museum of Natural History 4: 1–62.

Coombs, M.C. 1978b. Additional *Schizotherium* material from China, and a review of *Schizotherium* dentitions (Perissodactyla, Chalicotheriidae). American Museum Novitates 2647: 1–18.

Coombs, M.C. 1989. Interrelationships and diversity in the Chalicotheriidae. *In* R. Prothero and R.M. Schoch (editors), The evolution of Perissodactyla: 438–457. Oxford: Clarendon.

Coombs, M.C. 1998. Chalicotherioidea. *In* C.M. Janis, K.M. Scott, and L.L. Jacobs (editors), Evolution of Tertiary mammals of North America: 560–568. Cambridge: Cambridge University Press.

Cope, E.D. 1884. The vertebrata of the Tertiary formations of the West. Book 1. Report of the United States Geological Survey of the Territories 3: 1–1009.

Driesch, A. von den. 1976. A guide to the measurement of animal bones from archaeological sites. Peabody Museum of Natural History Yale University Bulletins 1: 1–137.

Eisenmann, V., M.T. Alberdi, C. De Giuli, and U. Staesche. 1988. Vol. 1. Methodology. *In* M. Woodburne and P. Sondaar (editors), Studying fossil horses: collected papers after the "New York International Hipparion Conference, 1981": 1–71. Leiden: Brill.

Fischer, K.H. 1977. Neue Funde von *Rhinocerolophiodon* (n. gen.), *Lophiodon*, und *Hyrachyus* (Ceratomorpha, Perissodactyla, Mammalia) aus dem Eozän des Geiseltals bei Halle (DDR). 1. Teil: *Rhinocerolophiodon*. Zeitschrift für Geologische Wissenschaften 5: 909–919.

Froehlich, D.J. 1999. Phylogenetic systematics of basal perissodactyls. Journal of Vertebrate Paleontology 19: 140–159.

Gazin, C.L. 1956. The geology and vertebrate paleontology of upper Eocene strata in the northeastern part of the Wind River Basin, Wyoming. Part 2. The mammalian fauna of the Badwater area. Smithsonian Miscellaneous Collections 131: 1–35.

Gingerich, P.D. 1974. Size variability of the teeth in living mammals and the diagnosis of closely related sympatric fossil species. Journal of Paleontology 48: 895–903.

Gingerich, P.D. 1991. Systematics and evolution of Early Eocene Perissodactyla (Mammalia) in the Clarks Fork Basin, Wyoming. Contributions from the Museum of Paleontology University of Michigan 28: 181–213.

Holbrook, L.T. 1999. The phylogeny and classification of Tapiromorph Perissodactyls (Mammalia). Cladistics 15: 331–350.

Holbrook, L.T. 2009. Osteology of *Lophiodon cuvier*, 1822 (Mammalia, Perissodactyla) and its phylogenetic implications. Journal of Vertebrate Paleontology 29: 212–230.

Hooker, J.J. 1989. Character polarities in early perissodactyls and their significance for *Hyracotherium* and infraordinal relationships. *In* D.R. Prothero and R.M. Schoch (editors), The evolution of perissodactyls: 79–101. Oxford: Clarendon.

Hooker, J.J. 1994. The beginning of the equoid radiation. Zoological Journal of the Linnean Society 112: 29–63.

Hooker, J.J., and D. Dashzeveg. 2003. Evidence for direct mammalian faunal interchange between Europe and Asia near the Paleocene-Eocene boundary. *In* S.L. Wing, P.D. Gingerich, and B. Schmitz (editors), Causes and consequences of globally warm climates in the Early Paleogene. Special Papers of the Geological Society of America 369: 479–500.

Hooker, J.J., and D. Dashzeveg. 2004. The origin of chalicotheres (Perissodactyla, Mammalia). Palaeontology 47: 1363–1386.

Huang, X.-S. 2002. New Eomoropid (Mammalia, Perissodactyla) remains from the middle Eocene of Yuanqu Basin. Vertebrata PalAsiatica 40: 286–290.

Li, C.-K., J. Meng, and Y.-Q. Wang. 2007. *Dawsonolagus antiquus*, a primitive lagomorph from the Eocene Arshanto Formation, Nei Mongol, China. Bulletin of Carnegie Museum of Natural History 39: 97–110.

Li, Q., and J. Meng. 2010. *Erlianomys combinatus*, a primitive myodont rodent from the Eocene

Arshanto Formation, Nuhetingboerhe, Nei Mongol, China. Vertebrata PalAsiatica 48: 133–144.

Lucas, S.G., and P.E. Kondrashov. 2004. Early Eocene (Bumbanian) perissodactyls from Mongolia and their biochronological significance. *In* S.G. Lucas, K.E. Zeigler, and P.E. Kondrashov (editors), Paleogene mammals. New Mexico Museum of Natural History and Science Bulletin 26: 215–220.

Lucas, S.G., and R.M. Schoch. 1989. Taxonomy and biochronology of *Eomoropus* and *Grangeria*, Eocene chalicotheres from the western United States and China. *In* D.R. Prothero and R.M. Schoch (editors), The evolution of perissodactyls: 422–437. Oxford: Clarendon.

McKenna, M.C., and S.K. Bell. 1997. Classification of mammals above the species level. New York: Columbia University Press.

Meng, J., C.-K. Li, X.-J. Ni, Y.-Q. Wang, and K.C. Beard. 2007a. A new Eocene rodent from the lower Arshanto Formation in the Nuhetingboerhe (Camp Margetts) area, Inner Mongolia. American Museum Novitates 3569: 1–18.

Meng, J., et al. 2007b. New stratigraphic data from the Erlian Basin: implications for the division, correlation, and definition of paleogene lithological units in Nei Mongol (Inner Mongolia). American Museum Novitates 3570: 1–31.

Mihlbachler, M.C. 2008. Species taxonomy, phylogeny, and biogeography of the Brontotheriidae (Mammalia: Perissodactyla). Bulletin of the American Museum of Natural History 311: 1–475.

Osborn, H.F. 1907. Evolution of mammalian molar teeth. New York: Macmillan.

Osborn, H.F. 1913. *Eomoropus*, an American Eocene chalicothere. Bulletin of the American Museum of Natural History 32(14): 261–274.

Peterson, O.A. 1919. Report upon the material discovered in the Upper Eocene of the Uinta Basin by Earl Douglass in the years 1908–1909, and by O.A. Peterson in 1912. Annals of Carnegie Museum 12: 40–168.

Prothero, D.R., and R.M. Schoch. 1989. Classification of the Perissodactyla. *In* D.R. Prothero and R.M. Schoch (editors), The evolution of perissodactyls: 530–537. Oxford: Clarendon.

Qiu, Z.-X., and B.-Y. Wang. 2007. Paracerathere fossils of China. Palaeontologia Sinica (C) 29: i–396.

Radinsky, L.B. 1964a. *Paleomoropus*, a new Early Eocene chalicothere (Mammalia, Perissodactyla), and a revision of Eocene chalicotheres. American Museum Novitates 2179: 1–28.

Radinsky, L.B. 1964b. Notes on Eocene and Oligocene fossil localities in Inner Mongolia. American Museum Novitates 2180: 1–11.

Radinsky, L.B. 1965. Evolution of the tapiroid skeleton from *Heptodon* to *Tapirus*. Bulletin of the Museum of Comparative Zoology 134: 69–106.

Remy, J.A., et al. 2005. A new chalicothere from the Pondaung Formation (late Middle Eocene of Myanmar). Comptes Rendus Palevol 4: 341–349.

Savage, D.E., D.E. Russell, and P. Louis. 1966. Ceratomorpha and Ancylopoda (Perissodactyla) from the Lower Eocene Paris Basin, France. University of California Publications in Geological Sciences 66: 1–38.

Schoch, R.M. 1989. A review of the tapiroids. *In* D.R. Prothero and R.M. Schoch (editors), The evolution of perissodactyls. Oxford: Clarendon, 298–320.

Shi, R. 1989. Late Eocene mammalian fauna of Huangzhuang, Qufu, Shandong. Vertebrata PalAsiatica 27: 87–102.

Simpson, G.G. 1941. Large Pleistocene felines of North America. American Museum Novitates 1136: 1–27.

Sun, B., L.-P. Yue, Y.-Q. Wang, J. Meng, J.-Q. Wang, and Y. Xu. 2009. Magnetostratigraphy of the Early Paleogene in the Erlian Basin. Journal of Stratigraphy 33: 62–68.

Swofford, D.L. 2001. PAUP* (phylogenetic analysis using parsimony [*and other methods] version 4.0b10). Sunderland, MA: Sinauer.

Thorley, J.L., and R.D.M. Page. 2000. RadCon: phylogenetic tree comparison and consensus. Bioinformatics 16: 486–487.

Tong, Y.-S., and J.-W. Wang. 2006. Fossil mammals from the Early Eocene Wutu Formation of Shandong Province. Palaeontologia Sinica (C) 28: i–195.

Tong, Y.-S., S.-H. Zheng, and Z.-D. Qiu. 1995. Cenozoic mammal ages of China. Vertebrata PalAsiatica 33: 290–314.

Wang, Y. 1995. A new primitive chalicothere (Perissodactyla, Mammalia) from the early Eocene of Hubei, China. Vertebrata PalAsiatica 33: 138–159.

Wang, Y.-Q., J. Meng, X.-J. Ni, and C.-K. Li. 2007. Major events of Paleogene mammal radiation in China. Geological Journal 42: 415–430.

Wilkinson, M. 1994. Common cladistic information and its consensus representation: reduced Adams and reduced cladistic consensus trees and profiles. Systematic Biology 43: 343–368.

Wilkinson, M. 1995. More on reduced consensus methods. Systematic Biology 44: 435–439.

Wilkinson, M. 2003. Missing entries and multiple trees: instability, relationships, and support in

parsimony analysis. Journal of Vertebrate Paleontology 23: 311–323.

Zdansky, O. 1930. Die alttertiären Säugetiere Chinas nebst stratigraphischen Bemerkungen. Palaeontologia Sinica (C) 6: 5–87.

Zhou, M.-Z., Z.-X. Qiu, and C.-K. Li. 1975. Some suggestions for unifying translation of nomenclature of the primative eutherian molar-teeth. Vertebrata PalAsiatica 13: 257–266.

Zong, G.-F., W.-Y. Chen, X.-S. Huang, and Q.-Q. Xu. 1996. Cenozoic mammals and environment of Hengduan Mountains region. Beijing: China Ocean Press.

APPENDIX 1

Measurements of skulls and mandibles of *Litolophus gobiensis* (mm)

(The skull and mandible measurements correspond with those used by Driesch (1976) and
Eisenmann et al. (1988). Asterisks (*) indicate approximate measurements.)

Skull and upper teeth	V16139	V16140-1	V1614-1
Distance between premaxillary tip and anterior border of P1	*83.5		*85.5
Palatal length	131.7		
Postpalatal length	*122.3		
Basilar length	*335.1	*331.2	*391.1
Palatal breadth in front of P2	*53.7		
Palatal breadth in front of M1	*64.0		
Palatal breadth in front of M3	*64.5		
Minimal muzzle breadth	51.2		
Bizygomatic breadth	*187.0		*192.8
Profile length (total length)	*375.2	*364.1	*432.3
Anteroposterior orbital diastema	*39.0	*31.5	43.2
Greatest breadth of the foramen magnum		25.7	*23.0
Height of the foramen magnum		*21.2	*20.6
Greatest breadth of the foramen condyles		*51.2	*53.9
Diastema between C and P1	30.1		*23.3
Diastema between P1 and P2	8.9	8.2	
C L	15.9		
C W	9.7		
C H	*31.6		
P1 L	11.9	11.6	
P1 W	6.6	6.1	
P2 L	11.9	*13.4	12.2
P2 W	10.8	11.2	10.6
P3 L	11.9	12.3	12.7
P3 W	14.3	14.7	15.1
P4 L	11.4	12.3	12.7
P4 W	16.1	16.5	17.0
M1 L	16.8		19.6
M1 W	19.0		20.3
M2 L	23.4		*23.5
M2 W	24.2		*24.0
M3 L	26.1	27.3	26.6
M3 W	29.4	29.5	29.8
P2–4	35.2		37.6
M1–3	66.3		69.7

APPENDIX 1
(Continued)

Mandible and lower teeth	V16149	V16150
Distance between the i1 and the back of condyle	268.1	250.5
Distance between the back of the alveole of m3 and the posterior edge of the ascending ramus	90.1	73.1
Height of the mandible at the condyle	84.1	80.0
Height of the mandible at the coronoid process	104.7	104.7
Height of horizontal ramus in front of m3	47.5	
Height of horizontal ramus in front of p2	41.0	
Length of the symphysis	*80.1	74.6
Diastema between c and p2	65.0	40.9
c L	10.5	13.3
c W	8.8	10.7
c H	21.7	
p2 L	12.6	12.9
p2 W	6.8	6.8
p3 L	12.4	13.2
p3 W	7.9	9.3
p4 L	12.1	13.2
p4 W	8.8	9.9
m1 L	16.0	18.2
m1 AW	10.0	11.9
m1 PW	11.1	12.6
m2 L	19.6	21.7
m2 AW	11.8	13.0
m2 PW	12.1	13.8
m3 L	29.2	32.2
m3 AW	13.2	14.4
m3 PW	12.9	13.8
p2–4	37.1	39.3
m1–3	64.8	72.1

APPENDIX 2
Measurements of incisors of *Litolophus gobiensis* (mm)

	I2			I3		i1	i2			i3	
	V16144.1	V16144.2	V16144.3	V16144.4	V16143	V 16147	V 16167.1	V 16167.2	V 16167.3	V 16167.4	V 16167.5
L	6.8	7.3	7.3	5.5	5.3	7.5	8.5	8.7	8.6	9.4	9.6
W	5.4	5.3	5.2	4.4	3.6		5.2	5.8	5.8	4.8	4.9
H	8.2	7.4	7.6	6.2	5.3	10.6	10	11	10.4	9.6	8.5

APPENDIX 3
Characters used in phylogenetic analyses

We use a different dental terminology (shown in figure 1) from most other authors, and any characters drawn from other authors' works have been modified to match our terminology.

1. P1: (0) present, (1) absent. Corresponds to character 20 of Hooker and Dashzeveg (2004).
2. Post P1 diastema: (0) present, (1) absent. Corresponds to character 52 of Hooker and Dashzeveg (2004), but states are different.
3. P2 protocone: (0) weak or absent, (1) prominent. New character.
4. Position of P2 protocone: (0) on transverse axis, (1) posteriorly. New character.
5. P2 protoloph: (0) absent, (1) weak, separated from protocone by a notch, (2) prominent. New character. Unordered.
6. P3 paraconule: (0) absent, (1) present. Corresponds to character 3 of Wang (1995).
7. P3 paracone and metacone: (0) well separated, (1) close together, (2) very close. Corresponds to character 51 of Hooker and Dashzeveg (2004). Ordered.
8. P3 protoloph: (0) absent, (1) present. New character.
9. P3 metaloph: (0) absent, (1) weak, not joining the ectoloph or the protocone, (2) lophid, joining the ectoloph in a low position, (3) lophid, joining the ectoloph in a high position. Corresponds to character 4 of Wang (1995), but states are different. Ordered.
10. P4 parastyle: (0) large, (1) small. New character.
11. P4 paraconule: (0) present, (1) absent. Corresponds to character 6 of Wang (1995).
12. P4 metaloph: (0) absent, (1) weak, not joining the ectoloph or the protocone, (2) lophid, joining the ectoloph in a low position, (3) lophid, joining the ectoloph in a high position. New character. Ordered.
13. Premolar metacone position relative to paracone: (0) posterior, (1) posterolingual. Corresponds to character 9 of Wang (1995).
14. Upper molar parastyle pointing: (0) essentially occlusally, (1) recurved strongly distally. Corresponds to character 42 of Hooker and Dashzeveg (2004).
15. Upper molar parastyle: (0) separated from the ectoloph, (1) fused together with ectoloph. New character.
16. M3 parastyle extends: (0) buccally, (1) strongly buccally, (2) anterobuccally. New character. Unordered.
17. Upper molar protocones: (0) do not extend posteriorly, (1) extend posteriorly, (2) strongly extend posteriorly. New character. Ordered.
18. Upper molar paraconules: (0) present, (1) absent. New character.
19. Anterior facet of upper molar paraconules: (0) convex, (1) flat. New character.
20. Upper molar paraconules: (0) do not extend posteriorly, (1) extend posteriorly. New character.
21. Upper molar mesostyles: (0) large, (1) small or variably developed, (2) lacking. Corresponds to character 11 of Hooker and Dashzeveg (2004). Ordered.
22. Upper molar metaloph: (0) transverse, (1) oblique. New character.
23. Upper molar metacone: (0) vertically implanted, (1) tilted slightly lingually, (2) tilted markedly lingually. Corresponds to character 44 of Hooker and Dashzeveg (2004). Ordered.
24. Upper molar paracone: (0) vertically implanted, (1) tilted slightly buccally, (2) tilted markedly buccally, (3) tilted lingually. Corresponds to character 45 of Hooker and Dashzeveg (2004), but states are different. Unordered.
25. Upper molar ectoloph between paracone and metacone: (0) slightly flexed buccally, (1) straight, (2) sharply flexed buccally. Corresponds to character 10 of Hooker and Dashzeveg (2004), but here is treated as unordered.
26. Upper molar buccal side of paracone: (0) conical, (1) prominent rib, (2) weak rib, (3) flat. New character. Unordered.
27. M1–2: (0) broader than long, (1) almost as long as broad, (2) longer than broad. Corresponds to character 21 of Hooker and Dashzeveg (2004), but states are different. Unordered.
28. M1–2 hypocone: (0) bunodont, (1) lophid, (2) slightly crescent. New character. Ordered.
29. The metacone and metaloph posterolaterally rotated on M3: (0) no, (1) yes. New character.
30. p1: (0) present, (1) absent. This corresponds to character 32 of Hooker and Dashzeveg (2004).
31. p3 paraconid: (0) weak, (1) prominent. New character.
32. p3 "metastylid": (0) absent, (1) weak, (2) prominent. New character. Unordered.
33. p3 entoconid: (0) absent, (1) weak to moderate. New character.
34. p4 "metastylid": (0) absent, (1) weak, (2) prominent. New character. Unordered.
35. p4 entoconid: (0) absent, (1) weak to moderate, (2) prominent. New character. Ordered.
36. m1–2 distal cingulum lingual to hypoconulid: (0) absent, (1) present. Corresponds to character 38 of Hooker and Dashzeveg (2004).
37. m1–2 hypoconulid: (0) cuspidate, (1) upward swollen, not cuspidate. New character.

38. m3 hypoconulid: (0) prominent, (1) small and narrow, (2) absent. Corresponds to character D14 of Holbrook (1999). Ordered.
39. m3 hypoconulid: (0) nearly as high as talonid, (1) much lower than talonid. New character.
40. m3 hypolophid: (0) notched, (1) complete. Corresponds to character 28 of Hooker and Dashzeveg (2004), but states are different.
41. Lower molar protolophid extends: (0) anteriorly, (1) anterolingually, (2) lingually. New character. Ordered.
42. Lower molar cristid obliqua attaches to trigonid: (0) nearer to protoconid than to metaconid, (1) midway between protoconid and metaconid, (2) nearer to metaconid than to protoconid. Corresponds to character 14 of Hooker and Dashzeveg (2004), but states are different. Ordered.
43. The m1–2 cristid obliqua attaches: (0) low on back wall of trigonid, (1) high on back wall of trigonid. New character.
44. Lower molar hypolophid: (0) nearly transverse, (1) more oblique. New character.
45. Lower molar "metastylid": (0) larger than or equal to metaconid, (1) smaller than metaconid, (2) absent. Corresponds to character 40 of Hooker and Dashzeveg (2004), but states are different. Ordered.
46. Lower canine: (0) small or equal compare to cheek teeth, (1) large, (2) absent. New character. Ordered.
47. Supraorbital foramen: (0) absent, (1) present. Corresponds to character C9 of Holbrook (1999).
48. Preorbital foramen: (0) above P2 or P3, (1) above M1 or M2. New character.
49. Posttympanic process: (0) long, (1) short. Corresponds to character C13 of Holbrook (1999).
50. Posterior part of the zygomatic arch: (0) reaching the same level as the upper border of the orbit, (1) always lower than the level of the upper border of the orbit. Corresponds to character 11 of Anquetin et al. (2007).
51. Braincase: (0) low, (1) high. Corresponds to character 12 of Anquetin et al. (2007).
52. Retromolar space on the maxilla: (0) present, (1) absent. Corresponds to character 22 of Anquetin et al. (2007).
53. Choanal opening: (0) anterior edge of M3, (1) at valley or posterior edge of M3, (2) far behind M3. Corresponds to character 23 of Anquetin et al. (2007), but states are different. Ordered.
54. Height of the mandibular corpus: (0) increasing posteriorly, (1) constant. Corresponds to character 30 of Anquetin et al. (2007).
55. Mandibular angle: (0) quite expanded ventrally, (1) expanded posteriorly, (2) not expanded. Corresponds to character 31 of Anquetin et al. (2007), but states are different. Unordered.
56. Retromolar space on the mandible: (0) absent, (1) present. Corresponds to character 32 of Anquetin et al. (2007).
57. Condyle position: (0) low, (1) high. New character.
58. Horizontal ramus of mandible: (0) shallow, (1) deep. New character.

APPENDIX 4
Data matrix

("A" refers to the score "0+1"; "B" refers to the score "1+2"; "C" refers to the score "1+3")

Taxon	1–10	11–20	21–30	31–40	41–50	51–58
Cardionlophus radinskyi	000-001100	0010000000	0110010000	0000000100	0000000000	000?0?0
Homogalax wuttuensis	?????11110	0300000000	0210010000	0?????1000	000000001?	????????
Lophiaspis maurettei	??10102101	1311000101	1220001001	??????1110	?1110111?0	???????1
Lophiodon remensis	1-10102100	1010000101	1221001001	0011001201	0??0001200	??????
Protomoropus gabuniai	??????1131	00010000--	2122100000	00110001??	?????????	???????
Paleomoropus jepseni	??????????	1100000002	1000000000	10??0111??	??????????	???????
Pappomoropus taishanensis	??????????	?100000020	1100001000	2?0101111??	?????0?????	??????0
Litolophus gobiensis	001A111120	0200100110	1121000011	2110A121110	0011111000	0??????
Eomoropus ulterior	0011211120	0100010110	1210001121	100102000110	112110??????	??????0
Grangeria canina	0011211120	?201001101	321010?001	10??021111??	1211110010	0?????1
"Grangeria" anarsius	??10101131	1301001100	13221101?0?	11001121010	111101110111	?????1
Eomoropus amarorum	??10101131	1300010110	1322110001	1001021001	1210011201	???1?0
Eomoropus quadridentatus	0110113013	0130010110	023231200?1	01B201????	12100111?1?	0
Eomoropus minimus (V 9911)	??????????	1300000001	0123220001	10??0112???	??????????	???????
SDM 84006	??112011130	1110010110	0123221001	1210??111??	??????????	???????
Eomoropus pawnyunti	??1000-20	21-2110010	023221000	2110??1211??	??????????	???????
Schizotherium avitum	1-11?0010	13011001?1	1102320011	212210111111	12210021110	0?????
Moropus elatus	1-111000130	113010200	1232221001	1-22110211111	0021211010	0
Ansiodon grande	1-1001A000	30010200C	2321001011	12--1211100	1111?000200	0
Hyrachyus eximius	0110201111	1A002010	2011000100	0000112-11	0002000010	10
Heptodon calciculus	0010100120	00020201	2011000110	1110000112	20?2?1011010	0